2012

Climatic effects of the Chicxulub impact ejecta

Devon Parkos
Purdue University

Marat Kulakhmetov
Purdue University

Brandon Johnson
Purdue University

Henry J. Melosh
Purdue University, jmelosh@purdue.edu

Alina A. Alexeenko
Purdue University - Main Campus, alexeenk@purdue.edu

Recommended Citation
Parkos, Devon; Kulakhmetov, Marat; Johnson, Brandon; Melosh, Henry J.; and Alexeenko, Alina A., "Climatic effects of the Chicxulub impact ejecta" (2012). *School of Aeronautics and Astronautics Faculty Publications.* Paper 44.
http://dx.doi.org/10.1063/1.4769724

Climatic Effects of the Chicxulub Impact Ejecta

Devon Parkos*, Marat Kulakhmetov*, Brandon Johnson†, Henry J. Melosh† and Alina Alexeenko*

*School of Aeronautics and Astronautics, Purdue University, West Lafayette, IN 47907, USA
†Department of Earth, Atmospheric, and Planetary Sciences, Purdue University, West Lafayette, IN 47907, USA

Abstract. Examining the short and long term effects of the Chicxulub impact is critical for understanding how life developed on Earth. While the aftermath of the initial impact would have produced harmful levels of radiation sufficient for eradicating a large portion of terrestrial life, this process does not explain the concurrent marine extinction. Following the primary impact, a large quantity of smaller spherules would de-orbit and re-enter the earths atmosphere, dispersed nearly uniformly across the planet. This secondary wave of debris would re-enter at high velocities, altering the chemical composition of the atmosphere. Furthermore, the combined surface area for the spherules would be much larger than for the original asteroid, resulting in considerably more potential reactions. For this reason, a new method was developed for predicting the total amount of toxic species produced by the spherule re-entry phase of the Chicxulub event. Using non-equilibrium properties obtained from direct simulation Monte Carlo (DSMC) methods coupled with spherule trajectory integration, the most likely cause of the observed marine extinction was determined.

Keywords: Astrophysics, Aeronomy, Chicxulub, Ejecta, Pollution
PACS: 51.10.+y, 96.30.Za, 92.60.Sz

INTRODUCTION

The evolution of life on Earth has been influenced by impacts of meteorites, comets, and asteroids. For example, global extinction at the end of the Cretaceous era, 65 million years ago, has been linked to the Chicxulub impact event [1]. Previous studies have suggested that the impact had both short and long term effects. Some studies suggest that Earth may have significantly cooled a few months after the impact due to blocking of solar radiation by the produced high altitude dust. Other studies suggest that impact produced a long term greenhouse effect by releasing carbon dioxide, sulfur-bearing gases, and water vapor. Hydrocode simulations by Pierazzo et al. [1] suggest that up to 3500 Gt of carbon dioxide, 1100 Gt of sulfur, and 600 Gt of water vapor were released into the atmosphere by the impact. Although the initial impact would have had drastic effects on the terrestrial ecosystems, it alone does not explain the marine extinction that occurred at the same time.

The Chicxulub impact event can be broken into several stages (Fig. 1). Initially, the asteroid approaches an area of Earth's surface composed primarily of silicate, covered with a layer of water approximately 500 m thick (Stage 1). During the impact a substantial mass of silicate is vaporized and ejected out of Earth's lower atmosphere, along with the water covering it (Stage 2). This vaporized matter will expand and cool in the upper atmosphere and begin to nucleate. After growing sufficiently large, the particles ultimately re-enter the Earth's atmosphere, distributed around the planet (Stage 3). Consequently, this mass is classified as distal ejecta [2]. In addition to the vaporized material, a considerable amount of solid silicate was ejected outward from the impact site (Stage 2). These particles would on average be larger and travel at lower velocities, affecting only the proximal environment. They are classified as local ejecta and would typically land within a few crater diameters of the epicenter.

Due to the global nature of the extinction event, the distal ejecta is of particular interest for this investigation. Calculations by Johnson and Melosh [2] suggest that for a 10 km diameter body striking the Chicxulub impact site at 21 km/s, the average and standard deviation of the distal ejecta will be 217 μm and 47 μm respectively. Smit [3] measured the deposited ejecta layers at distal sites, which were more than 7000 km from the Chicxulub crater and found that the average particle size was 250 μm, an observation consistent with Johnson and Melosh. Additionally, Smit determined that the spherules had a global density of approximately 20,000 per cm^2, corresponding to 1×10^{23} re-entering spherules total.

This work studies the effect of distal ejecta re-entry on atmospheric and oceanic environments. The spherules traveling at hypersonic speeds at altitudes between 60 and 140 km would have dissociated the air and produced nitric oxide and monatomic nitrogen, leading to the formation of stable toxins such as nitrous acid, nitric acid, and ammonia.

28th International Symposium on Rarefied Gas Dynamics 2012
AIP Conf. Proc. 1501, 1557-1564 (2012); doi: 10.1063/1.4769724

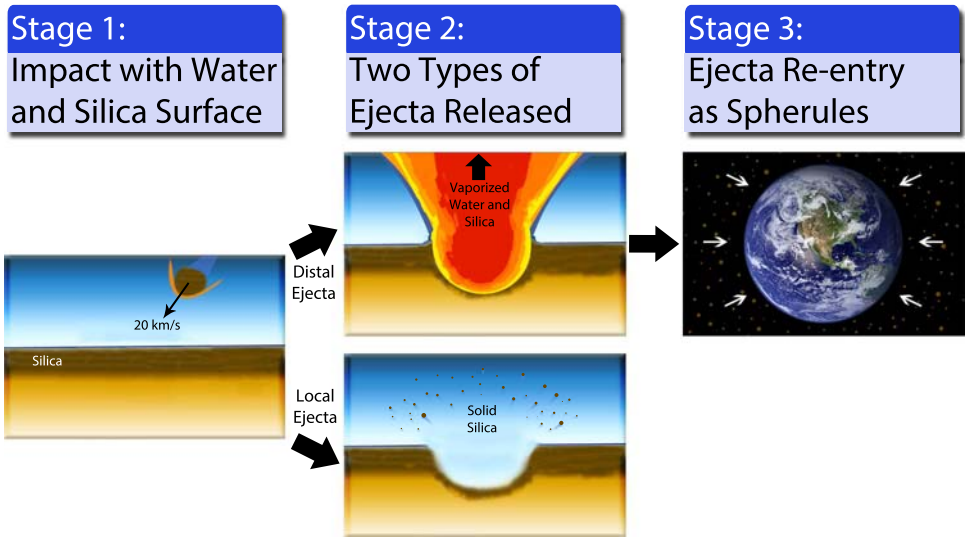

FIGURE 1. Schematic of various stages of Chicxulub impact.

In addition, the water vapor present in the upper atmosphere from the ejecta would lead to the presence of monatomic hydrogen. Lewis et al. [4] suggested that nitric oxide present in large quantities in the atmosphere would lead to the formation of acidic pollutants via the processes

$$\begin{aligned} NO + NO + O_2 &\rightarrow 2NO_2, \\ NO_2 + NO_2 &\rightarrow N_2O_4, \\ N_2O_4 + H_2O &\rightarrow HNO_2 + HNO_3. \end{aligned} \tag{1}$$

In high-enthalpy, non-equilibrium conditions such as during re-entry, the collisions with dissociated species will become more frequent, making the following reactions

$$\begin{aligned} NO + O &\rightarrow NO_2, \\ NO_2 + O &\rightarrow NO_3, \\ NO_2 + H &\rightarrow HNO_2, \\ NO_3 + H &\rightarrow HNO_3 \end{aligned} \tag{2}$$

more likely. The presence of monatomic nitrogen in a hydrogen-rich environment can lead to the formation of ammonia via the mechanisms

$$\begin{aligned} N + H &\rightarrow NH, \\ NH + H &\rightarrow NH_2, \\ NH_2 + H &\rightarrow NH_3. \end{aligned} \tag{3}$$

The pollutants would reach the surface as rain over the 10 days following the event. At concentrations of 100 ppm, nitrous acid can defoliate mature plants and is fatal to animals. The addition of 2×10^{40} molecules of NO related toxins to the ocean would significantly lower the pH of the topmost 75 m of oceans and could lead to the observed marine extinction [4]. Alternatively, the addition of the 2×10^{39} molecules of N related toxins would increase the pH level of the upper ocean and could also cause marine extinction [5, 6].

The distal ejecta started re-entry at 5 to 10 km/s [7], and in the process it compressed and heated the upper atmosphere. The atmospheric properties 10 minutes after the re-entry is shown in Fig. 2. Thermal radiation during the re-entry would approach 19 kW/m^2, enough to ignite woody biomass [7]. The large temperature increase of the atmospheric gases would cause some dissociation (Fig. 3) and result in 4.6×10^{37} dissociated nitrogen atoms and 2.9×10^{37} nitric oxide molecules spread throughout the atmosphere, but the total number of toxic particles is several orders of magnitude below the necessary value for the observed oceanic extinction. Therefore, it is crucial to consider the particles dissociated due to non-equilibrium conditions during the spherule re-entry phase.

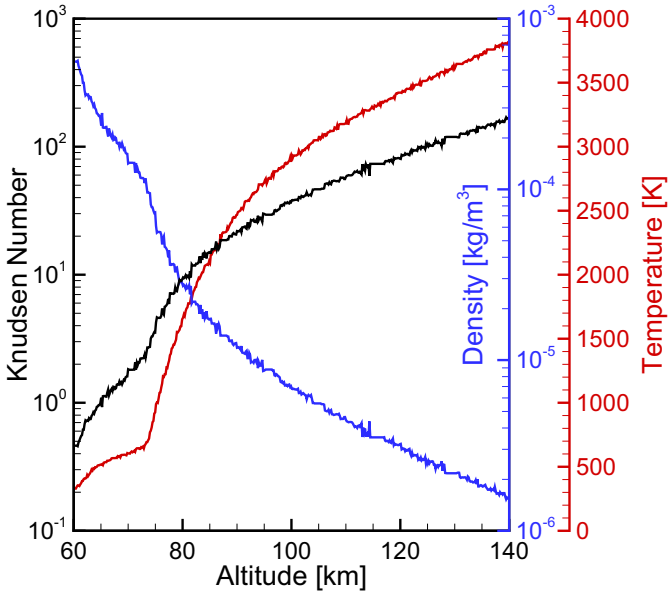

FIGURE 2. Atmospheric properties 10 minutes after the beginning of the distal ejecta re-entry (original data from Goldin [7]).

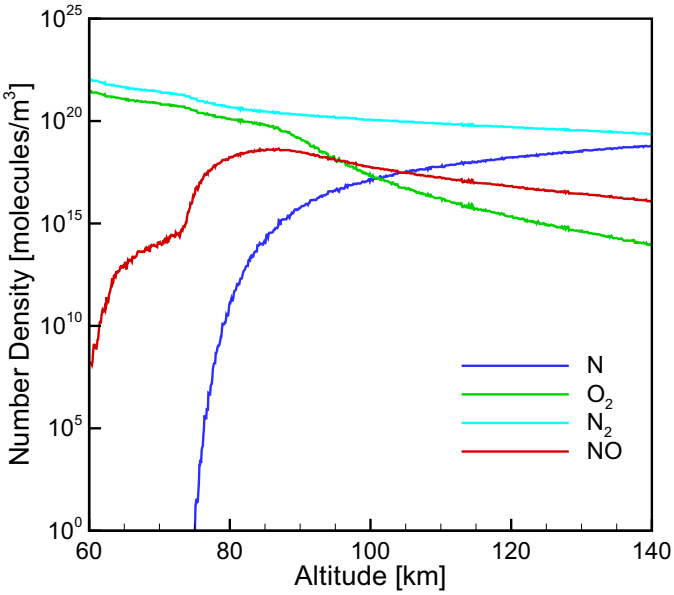

FIGURE 3. Equilibrium number densities of atmospheric species 10 minutes after the beginning of the distal ejecta re-entry.

MODELING APPROACH

DSMC Simulations

The non-equilibrium ejecta re-entry process is modeled using the direct simulation Monte Carlo (DSMC) method using the Statistical Modeling in Low Density Environment (SMILE) code [9]. The considered species were O, N, O_2, N_2, and NO. The rates for the considered reactions are from Hassan and Hash [10, 11]. The coefficients for the rates are highly uncertain, but they allow improvement beyond what is attainable from equilibrium calculations.

The domain was chosen to be large enough for accurate application of the boundary conditions. Of particular

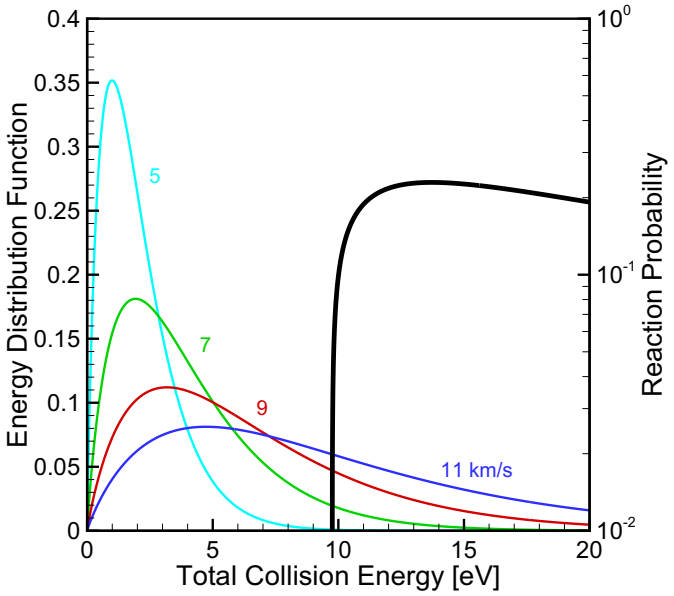

FIGURE 4. Reaction probability of diatomic nitrogen dissociation in air shown with the collision energy distribution functions at the stagnation point for various spherule velocities [8].

importance was the length of the domain behind the spherule, which needed to be sufficiently long to ensure that a low temperature and consequently low reaction probability was present at the exit.

The inlet conditions and concentrations were chosen to be representative of the steady-state conditions present shortly after the spherule re-entry phase began (See Fig. 2), which are conditions that the vast majority of the spherules would experience.

The necessary parameters for the investigation were extracted from the flow field data from the SMILE simulations (Fig. 5). By integrating the normal and shear pressures across the surface of the spherule, the drag force was obtained. To gain a particle generation rate for each species, the number fluxes were integrated around the perimeter of the domain. By repeating this procedure for each value of freestream velocity and density, the macroscale property variation with spherule velocity and altitude was ascertained.

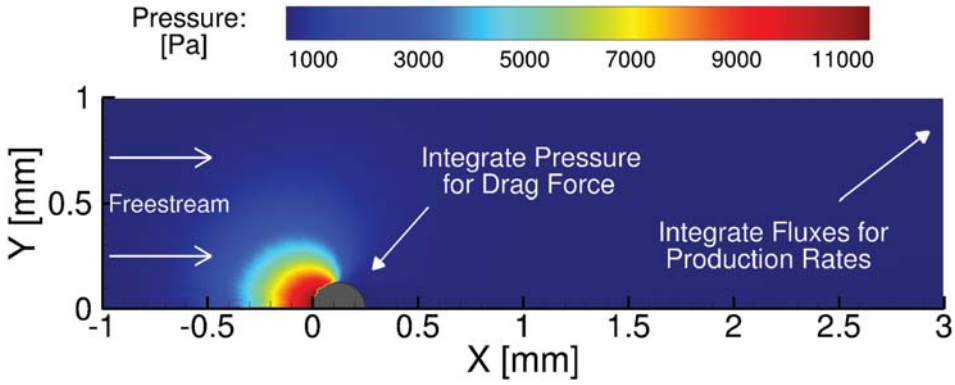

FIGURE 5. Schematic of flowfield for sample spherule re-entry. Pressure data is for re-entering spherule at 65 km altitude and 11 km/s velocity.

The flowfield shown in Fig. 6 illustrates the translational temperature. As can be seen, the translational temperature drops to below 1500 K at the right side of the domain, ensuring that few reactions are occurring.

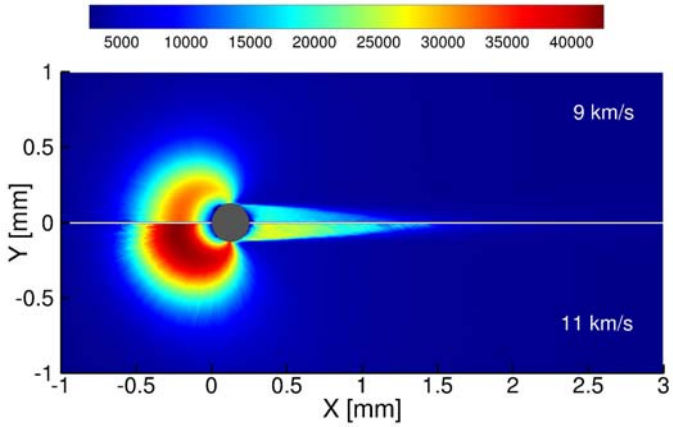

FIGURE 6. The translational temperature for a re-entering spherule at 65 km altitude.

Figure 7 shows the number density of nitric oxide, one of the species of interest. The spherule clearly cause significant production of NO, and large fraction of those particles persist until the temperature decreases.

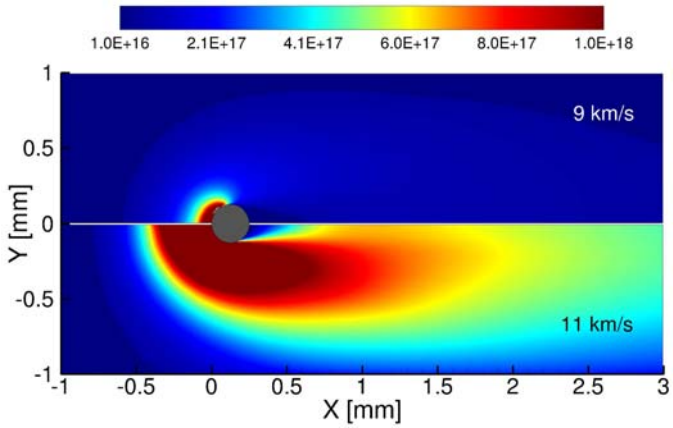

FIGURE 7. The nitric oxide number density for a re-entering spherule at 65 km altitude.

Figure 8 shows the number density of monoatomic nitrogen, the other species of interest. The spherule again causes significant production, and even more of the particles survive to exit the domain.

Trajectory Integration

The spherule diameter was chosen to be 250 μm, based on the ground measurements [3]. The initial velocity was chosen to be 8 km/s, angled $\pi/4$ downward from the horizontal direction, representative of the average conditions [7] experienced by a re-entry spherule. The integration was performed using a 4th order, explicit Runge-Kutta method. The integration was terminated when the velocity decreased to 5 km/s, sufficiently low to cause no appreciable reactions involving the species of interest (Fig. 4).

To calculate the values for the drag force and the species production rates, bilinear interpolation was performed using the DSMC results for various altitudes and velocities. Higher order schemes do not consistently reproduce the monotonic behavior that must be physically true (e.g. an increase in drag force from an increase in either velocity or density).

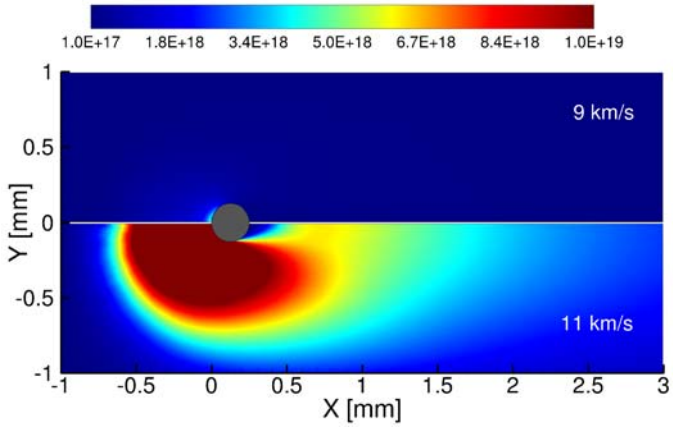

FIGURE 8. The monoatomic nitrogen number density for a re-entering spherule at 65 km altitude.

RESULTS AND DISCUSSION

A total of sixteen DSMC cases were ran, for all combinations of the altitudes 66, 86, 114, and 134 km and the velocities 5.5, 7.3, 9.7, and 11.5 km/s. These values were chosen using Gauss Legendre quadrature for the range of altitudes from 60 to 140 km and the range of velocities from 5 to 12 km/s. The values for the drag coefficient resulting from the surface forces in the DSMC simulations are shown in Fig. 9, compared with an existing model from Crowe [12]. As can be seen, the values match relatively closely to the expected value of 2 for high velocities. The DSMC data points deviate from the Crowe fit for the lowest altitude of 66 km. The Knudsen number at that altitude is outside the range for which the Crowe fit was formulated, so the observed deviation is expected.

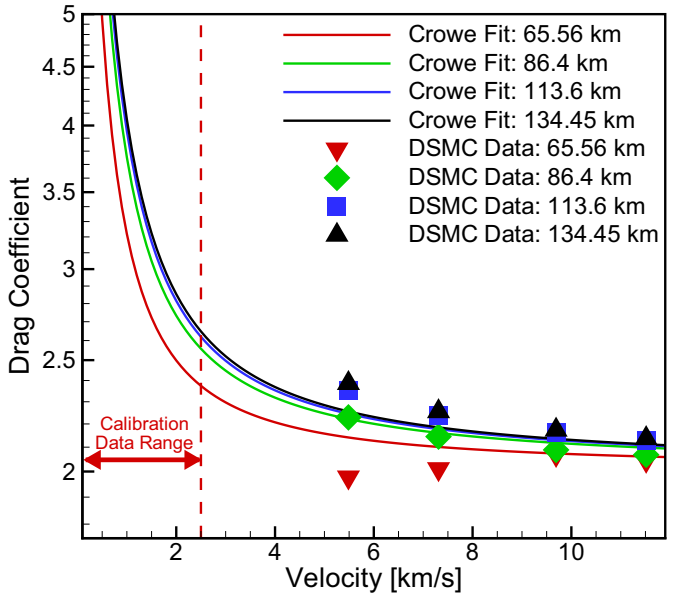

FIGURE 9. The drag coefficient predicted by the SMILE simulations compared to the model provided by Crowe [12].

The values for the species production rate of nitric oxide obtained from the number flux of the DSMC flowfields are shown in Fig. 10. The rates consistently increase with velocity and consequently increased temperature, as expected. For the lowest velocity, the lowest altitude data point has a lower rate than the other altitudes, due to the high pressure preventing the nitrogen from as readily dissociating. This effect is less pronounced at the higher velocities.

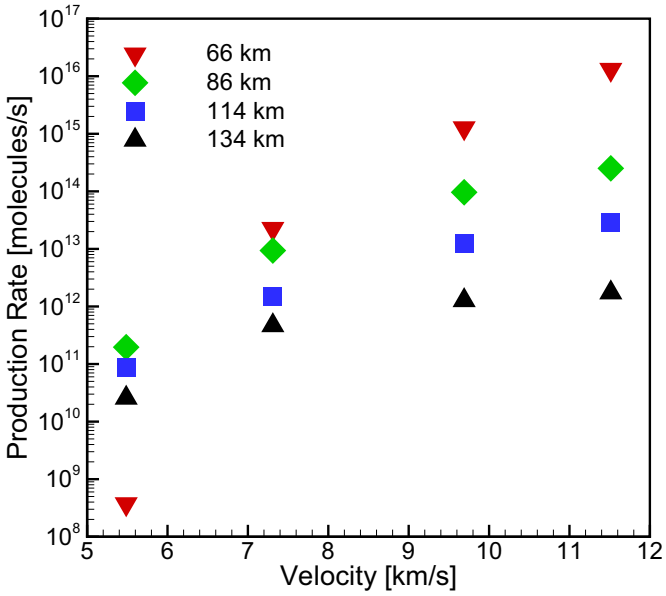

FIGURE 10. The nitric oxide production for the simulated altitudes and velocities.

By integrating the production rate divided by the velocity and the altitude dependent surface area across which it is spread, the altitude dependent density contribution due to the re-entry of one spherule is obtained, given by the expression

$$n_i = \frac{\dot{N}}{v} \frac{1}{4\pi(r_e + h)^2}, \tag{4}$$

where N is the number of particles, v is the spherule velocity, r_e is the radius of the earth, and h is altitude. Multiplying by the total number of spherules leads to the density distribution shown in Fig. 11. Integration across all altitudes yields the total number density of each species contributed by all the spherules, shown in Table 1.

This total number of particles from both equilibrium and non-equilibrium calculations represents the highest possible contribution to oceanic toxicity. In reality, the number of particles that survive to reach the ocean will be lower, due to the slow decay of the toxic species. In general, the overall production at the end of the spherule re-entry phase provides insight into which species is more likely to contribute to the observed oceanic extinction. The only species produced in quantities sufficient for extinction is atomic nitrogen (nearly three times required amount), therefore ammonia toxicity is best choice to investigate further.

By calculating the fraction of atomic nitrogen and nitric oxide that become ammonia and nitrogen dioxide respectively, the long-term lifespan of the toxins will be more apparent. However, this will need to be coupled with atmospheric transport of the various species and rates for absorption into cloud moisture leading to acid rain. A complete analysis of this process is beyond the scope of this paper.

TABLE 1. Non-equilibrium and equilibrium species production totals for the 60 to 140 km range of altitudes.

Species Name	Symbol	Non-Equilibrium Molecules	Equilibrium Molecules	Extinction Threshold
Atomic Oxygen	O	5.2×10^{40}	1.2×10^{39}	–
Atomic Nitrogen	N	5.4×10^{39}	4.6×10^{37}	2×10^{39}
Nitrogen Monoxide	NO	5.8×10^{35}	2.9×10^{37}	2×10^{40}

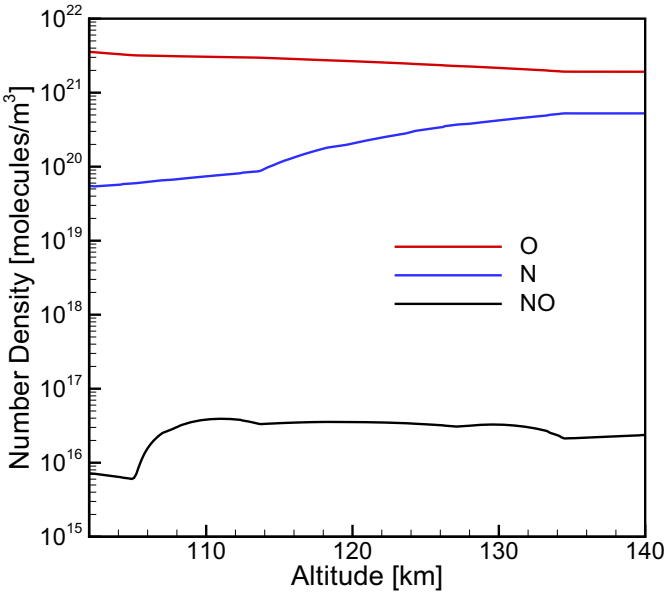

FIGURE 11. The number density of various species added to the atmosphere by the re-entering spherules.

CONCLUSION

Based on equilibrium and non-equilibrium production of toxic species from the re-entry spherules, the most feasible route for causing the observed marine extinction would be through the production of ammonia. The equilibrium concentrations of the considered toxin causing species were far too low to be responsible for the observed extinction, and only the concentration of monatomic nitrogen due to non-equilibrium calculations was sufficient.

Future work includes more accurately representing the distribution of spherule conditions (e.g. variable diameter, initial velocity, etc.) and improving the interpolation of macroscale properties between the DSMC data points. To determine what fraction of the produced monatomic nitrogen will form ammonia and what portion of the ammonia will ultimately reach the ocean, a large scale simulation of the chemically reacting atmosphere after the re-entry phase will need to be performed, coupled with atmospheric transport and acid rain formation rates.

REFERENCES

1. E. Pierazzo, D. Kring, and J. Melosh, *J. Geophys. Res.* **103**, 28–625 (1998).
2. B. Johnson, and J. Melosh, *Icarus* **217**, 416–430 (2012).
3. J. Smit, "The global stratigraphy of the Cretaceous-Tertiary boundary impact ejecta," Annu. Rev. Earth Pl. Sc., 1999, pp. 75–113.
4. J. Lewis, H. Watkins, H. Hartman, and R. Prinn, *Geological implications of impacts of large asteroids and comets on the earth* (1982).
5. D. Randall, and T. Tsui, *Mar. Pollut. Bull.* **45**, 17–23 (2002).
6. G. Lemarie, D. Coves, G. Dutto, E. Gasset, and J. Ruyet, "Chronic Toxicity of Ammonia for European Seabass (Dicentrarchus Labrax) Juveniles," International Congress on the Biology of Fishes, 1996.
7. T. Goldin, *Atmospheric Interactions During Global Deposition of Chicxulub Impact Ejecta*, Ph.D. thesis, University of Arizona (2009).
8. C. Park, *Nonequilibrium Hypersonic Aerothermodynamics*, Wiley-Interscience Publications, John Wiley and Sons, 1990.
9. M. Ivanov, A. Kashkovsky, S. Gimelshein, G. Markelov, A. Alexeenko, Y. Bondar, G. Zhukova, S. Nikiforov, and P. Vashenkov, "SMILE system for 2D/3D DSMC computations," Proceedings of 25th International Symposium on Rarefied Gas Dynamics, St. Petersburg, Russia, 2006, pp. 21–28.
10. H. Hassan, and D. Hash, *Phys. Fluids* **5**, 738–744 (1993).
11. D. Hash, and H. Hassan, "Direct Simulation of Diatomic Gases Using the Generalized Hard Sphere Model," AIAA 31st Aerospace Sciences Meeting and Exhibit, 1993, pp. 1–12.
12. C. Crowe, M. Sommerfeld, and Y. Tsuji, *Multiphase Flows with Droplets and Particles*, CRC Press, 1998.